Electronic Supplementary Material (ESI) for Analyst.

Electronic Supplementary Information

Collision Cross Sections and Ion Structures: Development of a General Calculation Method via High-quality Ion Mobility Measurements and Theoretical Modeling

Jong Wha Lee,[a] *Kimberly L. Davidson,*[b] *Matthew F. Bush,*[b] *Hugh I. Kim**[c]

[a]Center for Analytical Chemistry, Division of Chemical and Medical Metrology, Korea Research Institute of Standards and Science (KRISS), Daejeon 34113, Republic of Korea

[b]Department of Chemistry, University of Washington, Box 351700, Seattle, WA 98195-1700, United States

[c]Department of Chemistry, Korea University, Seoul 02841, Republic of Korea

*To whom correspondence should be addressed: E-mail: hughkim@korea.ac.kr

TABLE OF CONTENTS

METHODS

Materials and sample preparation. General sample preparation procedure for drift-tube ion mobility mass spectrometry (DTIM-MS) experiments is available in the main text. As exceptions to the procedure, carbazole was dissolved in pure methanol to a 10 mM concentration. 5,7-Dichloro-8-quinolinol was not soluble at 1 mM concentration in any of the solvent compositions tested and a saturated solution in a 49.5/49.5/1.0 water/acetonitrile/formic acid solvent mixture was prepared and diluted 1,000 ~ 10,000 fold for the experiments. Guanine and cucurbit[6]uril were solubilized in a 50/50 water/formic acid solution.

Calibrants for travelling-wave ion mobility mass spectrometry (TWIM-MS) experiments were purchased from Sigma-Aldrich (SA; Saint Louis, MO, USA) or Tokyo Chemical Industries (TCI; Tokyo, Japan), and their names, suppliers, and product numbers are: polyalanine (SA, P9003); glycylglycine hydrochloride monohydrate (TCI, G0125); Gly-Gly-Gly (SA, G1377); glycylglycylglycylglycine (TCI, G0127); Gly-Gly-Gly-Gly-Gly (SA, G5755); Gly-Gly-Gly-Gly-Gly-Gly (SA, G5630).

Traveling-wave ion mobility mass spectrometry (TWIM-MS). TWIM-MS experiments were performed using a standard Synapt G2-S*i* quadrupole ion mobility orthogonal time-of-flight mass spectrometer equipped with a standard Waters Z-Spray electrospray ionization source (Waters Corporation, Wilmslow, UK). A trap cell gas flow of 2.0 mL/min (argon), helium cell gas flow of 180.0 mL/min (helium), and IM cell gas flow (nitrogen) of 90.0 mL/min (nitrogen) were used for the experiments, resulting in pressures of ~4.11 mbar inside the helium cell and ~3.07 mbar inside the IM cell. Previously published collision cross section (CCS) values for polyalanines (n = 3 – 9)[1] or oligoglycines (n = 2 – 6)[2] were used for CCS calibration.[1] Three different combinations of travelling wave velocity and height were

used and the resulting CCS values were averaged and reported.

Computational modeling. Due to the rigidity of the ions studied, calculated ion CCS values were generally influenced insignificantly by the choice of ionization site and conformation. However, extensive computation was performed to obtain the most reliable theoretical ion structures. Briefly, a combination of molecular mechanics conformational search using Avogardro 1.2.0 and geometry optimization using Q-Chem 4.3 (Q-Chem, Inc., Pleasanton, CA, USA) was used, except for the 18-crown-6 and cucurbit[*n*]uril complexes.[3, 4] For ions other than the 18-crown-6 and cucurbit[*n*]uril complexes, all nitrogen and oxygen atoms were considered as possible protonation sites and sampled structures with energies of 20 kJ/mol or smaller, with respect to the most stable conformation, were optimized at the B3LYP level of theory with the 6-311G** basis set. For the 18-crown-6 and cucurbit[*n*]uril complexes, 1,000 cycles of simulated annealing were performed for conformation sampling using GROMACS 4.5.5,[5] and the resulting structures were analyzed by clustering. Due to the symmetry of 18-crown-6 and cucurbit[*n*]uril ions the clustered structures were manually examined and those with essentially identical structures were considered to belong to identical clusters. The representative structure in each cluster was geometry optimized at the B3LYP level of theory with the 6-311G** basis set (18-crown-6) or 6-31G basis set (cucurbit[*n*]uril) using Q-Chem. Extra sampling of possible structures that were inaccessible with the aforementioned methods was performed manually and geometry optimized. Frequency calculations were performed to ensure the absence of imaginary frequencies, and the structures were further optimized with a larger grid if necessary to remove imaginary frequencies. It was not possible to perform frequency calculations for the cucurbit[7]uril ions due to the large memory requirements. Final candidate structures with zero-point corrected energies of 10 kJ/mol or smaller, with respect to the most stable conformation, were selected and subjected to CCS calculations.

CCS calculation details. For the hard-sphere calculations, i.e., projection approximation (PA)[6] and exact hard-spheres scattering (EHSS),[7] 250,000 Monte Carlo trajectories (*inum*) were employed, and a maximum of 30 successive reflections (*inor*) were allowed. For the trajectory (TJ) calculations, ten complete cycles of mobility calculations (*itn*) were performed with 40 points of velocity integration (*inp*) and 100 points of impact parameter (*imp*) integration.

In molecular modeling, it is typically recommended to use partial charges that are compatible with a force field (FF). However, CCS calculation results were minimally dependent on the use of different partial charge assignment schemes. Therefore, for CCS calculations in this study, FF-compatible partial charges were used if straightforward and automatic tools were available, whereas Mulliken partial charges were used in other cases. In the case of CHARMM general force field (CGENFF), straightforward assignment of partial charges is relatively difficult and Mulliken charges were used. For general Amber force field (GAFF), AM1-bcc charges calculated using the *antechamber*[8] module of AmberTools 14 or RESP charges calculated using the R.E.D. Server Development[9, 10] were employed. The MM3 FF uses dipole-dipole interactions to describe the electrostatic interactions, but it has been noted previously that using atom-centered partial charges can provide similar results.[11] Thus, Mulliken charges were employed for the MM3 FF. Both electrostatic potential (ESP) and Mulliken charges were used during parameter development of the Merck molecular force field (MMFF94) FF.[12] Therefore, Mulliken charges were also used for the MMFF94 FF in this study, with the exception of proteins, for which uniformly distributed charges were used (see below).

The Exp-6 potential has a unique characteristic in that the potential becomes negatively infinite as the interatomic distance reaches zero. This is because the exponential repulsive

term converges to a finite constant, while the 6th-inverse-power attractive term diverges as the interatomic distance reaches zero. To test the effect of this unwanted property, a switched potential containing a 12th-inverse-power repulsive term was employed at close interatomic distances. The differences in calculation results were found to be negligible and, thus, the original Exp-6 potentials without the switching potential were used in this study.

Optimization of scaling factors for combined van der Waals (vdW) potential-forms and their parameters. Two terms characterize the van der Waals (vdW) interactions between interaction partners in a classical vdW potential, with each related to the distance or energy. The 12-6 Lennard-Jones (LJ) potential can be expressed in two equivalent ways:

$$V(r_i) = 4\varepsilon_i[(\frac{\sigma_i}{r_i})^{12} - (\frac{\sigma_i}{r_i})^6] = \varepsilon_i[(\frac{r_i^*}{r_i})^{12} - 2(\frac{r_i^*}{r_i})^6]. \text{ (S1)}$$

Here, r_i is the distance between the atoms, ε_i is the well depth, σ_i is the distance at which the potential is zero, and r_i^* is the distance at the potential minimum. The original MOBCAL code[13] calculates the 12-6 LJ potential based on σ_i, but the results are identical to those obtained based on r_i if $r_i = 2^{1/6}\sigma_i$.

The Exp-6 potential of the MM3 FF (abbreviated Exp-6(MM3); Eq. S2)[11] and the Buffered-14-7 potential (Buf-14-7; Eq. S3)[14] express the interaction distance in terms of minimum-energy distance (r_i):

$$V(r_i) = \varepsilon_i[1.84 \times 10^5 \exp\left(-\frac{12r_i}{r_i^*}\right) - 2.25(\frac{r_i^*}{r_i})^6], \text{ (S2)}$$

$$V(r_i) = \varepsilon_i(\frac{1.07r_i^*}{r_i+0.07r_i^*})^7 \left(\frac{1.12{r_i^*}^7}{{r_i}^7+0.12{r_i^*}^7} - 2\right). \text{ (S3)}$$

Therefore, the parameters in Eqs. S1–S3 represent identical physical properties and can be applied to other types of vdW potential without harming their physical context. As a note, ε_i in Eqs. S1 and S3 represents the minimum energy (energy at r_i^*) while in Eq. S2 the

minimum energy is 1.1195ε_i. This was taken into account during optimizing the scaling factors (δ_{dist}, and δ_{ener}) for the distance-related parameters (σ_i or r_i^*) and the energy-related parameters (ε_i), but did not influence the overall results because the net effect is similar to changing δ_{ener}.

Alternative forms of the LJ potential include the 7-6, 9-6,[15] 15-6, and 18-6 potentials, which can be expressed as:

$$V(r_i) = \varepsilon_i[6(\frac{r_i^*}{r_i})^7 - 7(\frac{r_i^*}{r_i})^6], \text{(S4)}$$

$$V(r_i) = \varepsilon_i[2(\frac{r_i^*}{r_i})^9 - 3(\frac{r_i^*}{r_i})^6], \text{(S5)}$$

$$V(r_i) = \varepsilon_i[\frac{2}{3}(\frac{r_i^*}{r_i})^{15} - \frac{5}{3}(\frac{r_i^*}{r_i})^6], \text{(S6)}$$

$$V(r_i) = \varepsilon_i[\frac{1}{2}(\frac{r_i^*}{r_i})^{18} - \frac{3}{2}(\frac{r_i^*}{r_i})^6], \text{(S7)}$$

where Eqs. S4, S5, S6, and S7 are the 7-6, 9-6, 15-6, and 18-6 LJ potentials, respectively. The coefficient in front of each term (e.g. 6 and −7 in case of Eq. S4) has been chosen so that the energy at r_i^* becomes the minimum energy ε_i. Therefore, the physical contexts of ε_i and r_i^* in Eqs. S4-S7 are identical to those in Eqs. S1–S3.

Exp-6-type potentials can be generally expressed as:

$$V(r_i) = A\exp\left(-B\frac{r_i}{r_i^*}\right) - C(\frac{r_i^*}{r_i})^6, \text{(S8)}$$

where A, B, and C are coefficients that can be chosen arbitrarily. Consequently, a much greater variety of the Exp-6 potential is possible and arbitrary choices may yield potentials with physically unrealistic shapes. Therefore, we employed Exp-6-type potentials used in two other FFs, the MM2 and Dreiding FFs (abbreviated Exp-6(MM2) and Exp-6(Dreiding),

respectively).[16, 17]

$$V(r_i) = \varepsilon_i[2.90 \times 10^5 \exp\left(-\frac{12.5 r_i}{r_i^*}\right) - 2.25(\frac{r_i^*}{r_i})^6] \quad \text{(S9)}$$

$$V(r_i) = \varepsilon_i[\exp(12.0) \exp\left(-\frac{12 r_i}{r_i^*}\right) - 2(\frac{r_i^*}{r_i})^6] \quad \text{(S10)}$$

Eqs. S9 and S10, respectively, are the Exp-6(MM2) and Exp-6(Dreiding) potentials. As a note, the minimum energy for the Exp-6(MM2) potential (Eq. S9) is 1.1693ε_i. This was taken into account during parameter optimization but did not influence the overall results because the net effect is similar to changing δ_{ener}.

Optimization of mixed vdW potentials was performed similarly to the unmodified FF potentials. However, a greater range of δ_{dist} and δ_{ener} values (0.70 – 1.30) was screened. A summary of the vdW parameters and potential-form combinations is available in Table S8.

Calculation of protein CCS. Biomacromolecules with various sizes were selected and their crystal structures were obtained from the protein data bank (PDB). Melittin (PDB code: 2MLT), insulin (PDB code: 3E7Y), ubiquitin (PDB code: 1UBQ), trypsin (PDB code: 4I8H), and tetrameric concanavalin A (PDB code: 1bxh) were used for calculations. Crystal waters and other non-protein components were removed and a single polypeptide chain (except for tetrameric concanavalin A) was extracted using Visual Molecular Dynamics 1.9.[18] Missing hydrogen atoms were added to the extracted polypeptides using GROMACS 4.5.5.[5] Open Babel 2.3.2[19] was then used to convert the resulting .pdb file into an .sdf file, and atom type assignments were performed using sdf2xyz2sdf software.[20] An in-lab python code was used to automatically append appropriate MMFF94 vdW parameters to input mfj files for MOBCAL. Uniformly-distributed charges were used when ion-induced dipole interactions were included, and a total charge of +4, +4, +6, +9, and +20 was assigned to melittin, insulin,

ubiquitin, trypsin, and tetrameric concanavalin A, respectively. Computation for the largest ion investigated, tetrameric concanavalin A (~100 kDa), required ~7 h without ion-induced dipole interactions and ~16 h with ion-induced dipole interactions, using a single core of our server equipped with an Intel i5-4670K processor.

DISCUSSION

CCS calibration using TWIM-MS. TWIM-MS requires calibration of experimental arrival times with previously reported CCS values to obtain the CCS of a desired analyte.[21, 22] The most popular calibrant for small ions is polyalanine,[1] and both linear or power-fit calibration curves may be used.[22] Fig. S3 and Table S3 compare the CCS values from TWIM-MS experiments with experimental CCS values from DTIM-MS experiments. It is observed that polyalanine calibration gives reasonable CCS values if the CCS values of the analytes are within the range of CCSs covered by the calibrant. However, for ions that are smaller than the smallest polyalanine calibrant (CCS = 89 $Å^2$), the calibrated CCS deviates greatly with a maximum error of ~50% when linear calibration curves were used. Power-fit calibration curves improve the calibrated CCS, and the errors are significantly smaller than those obtained using linear calibration curves, which is similar to previous reports.[1, 23] However, large errors up to 15% are still observed for small ions. Furthermore, the errors are mostly positive, suggesting that systematic errors are present.

To probe the effect of calibrant size-mismatching on calibrated CCS values, previously reported CCS values for oligoglycines[2] (tabulated in http://www.indiana.edu/~clemmer/), which are much smaller than polyalanines (62–107 $Å^2$), were used for calibration. It was observed that the relative errors for most ions decreased to below 10% (Fig. S3). Furthermore, the calibrated CCS values deviate in both the positive and negative direction, and the dependence on the calibration-curve selection (linear versus power) becomes small. This shows that calibrant size-mismatching was an important contribution to the errors that were observed with polyalanine calibrants. However, the relative errors obtained with oligoglycines are still large and their origins should be understood. Notably, the oligoglycine calibration curves showed relatively small R^2 values (~0.987), while those for the

polyalanines displayed a much better correlation (R^2 ~0.997). This suggests that the correlation between helium CCS values and arrival times measured using a TWIM-MS instrument is more complex for oligoglycines than polyalanines. This complexity may originate from either the use of TWIM-MS itself, or the use of nitrogen as the drift gas. It has been reported previously that molecular properties can affect the quality of CCS calibration,[21, 24] due to the differences between the ion-neutral interactions in helium and nitrogen.[24] In a previous study, TWIM-MS experiments were performed using helium as the drift gas and oligoglycines as the calibrants.[25] The calibrated CCS for amantadine (**4** in Fig. S3) in the referenced study was 66.40 Å^2 (−1.3%),[25] whereas the calibrated CCS in this study is 69.50 Å^2 (+3.4%; Table S3). Therefore, we can estimate that roughly 4.7%p of the errors to originate from the conversion of arrival times in nitrogen to CCS values in helium. As the importance of specific ion-neutral interactions becomes greater for small ions,[23] we infer that this contribution to the calibration error will be smaller for ions with larger sizes.

Fig. S1. Structures of small molecules used in this study.

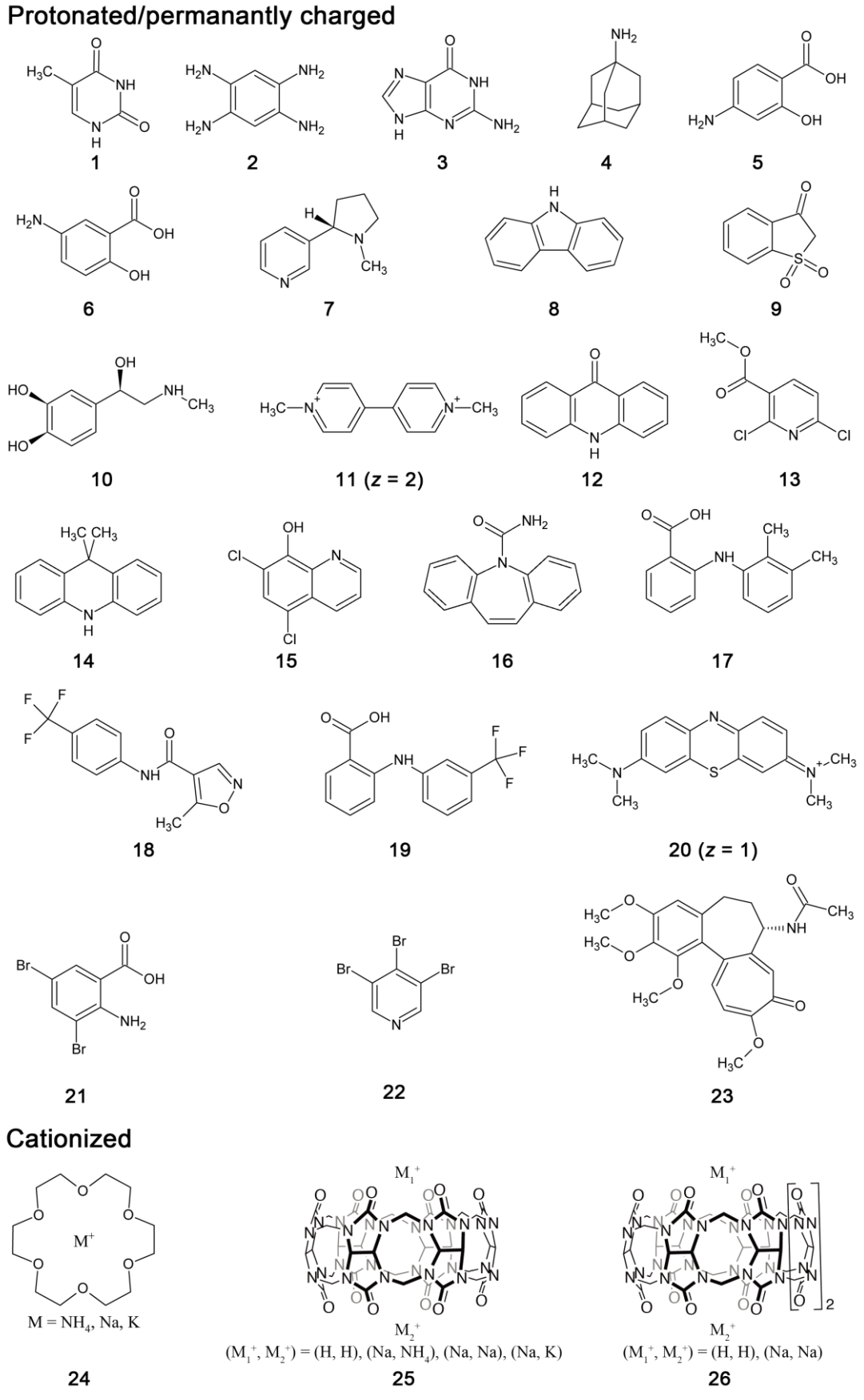

Fig. S2. Comparison between experimental CCS values measured using an Agilent 6560 ion mobility quadrupole time-of-flight instrument[26, 27] located at Korea University (KU), Seoul, Korea, and a Synapt G2 HDMS quadrupole ion mobility time-of-flight instrument located at the University of Washington (UW), Seattle, WA, USA, in which the travelling-wave ion mobility cell was replaced with an RF-confined drift cell.[28] The red and blue error bars indicate the experimental standard deviations for measurements using the Agilent and the modified Synapt instrument, respectively.

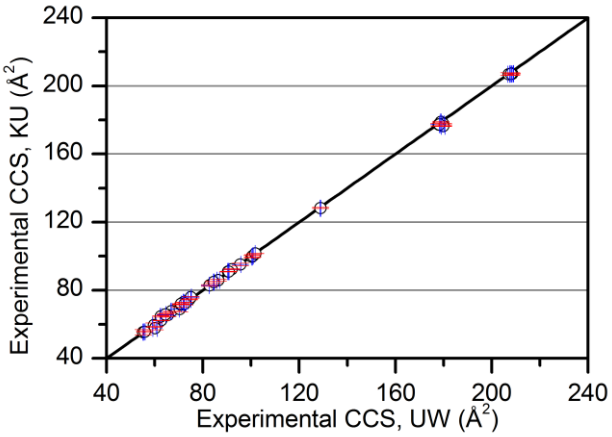

Fig. S3. Relative error between CCS obtained using TWIM-MS, either using polyalanines or oligoglycines as the calibrant, and either using a linear-fit or a power-fit calibration curve, with respect to experimental CCS from DTIM-MS experiments. The red dashed lines represent the range of CCS values covered by the calibrants (89–170 Å^2 for polyalanine and 62–107 Å^2 for oligoglycine).[1, 2] The errors were calculated using propagation of error from the standard deviations. The data are summarized in Table S3.

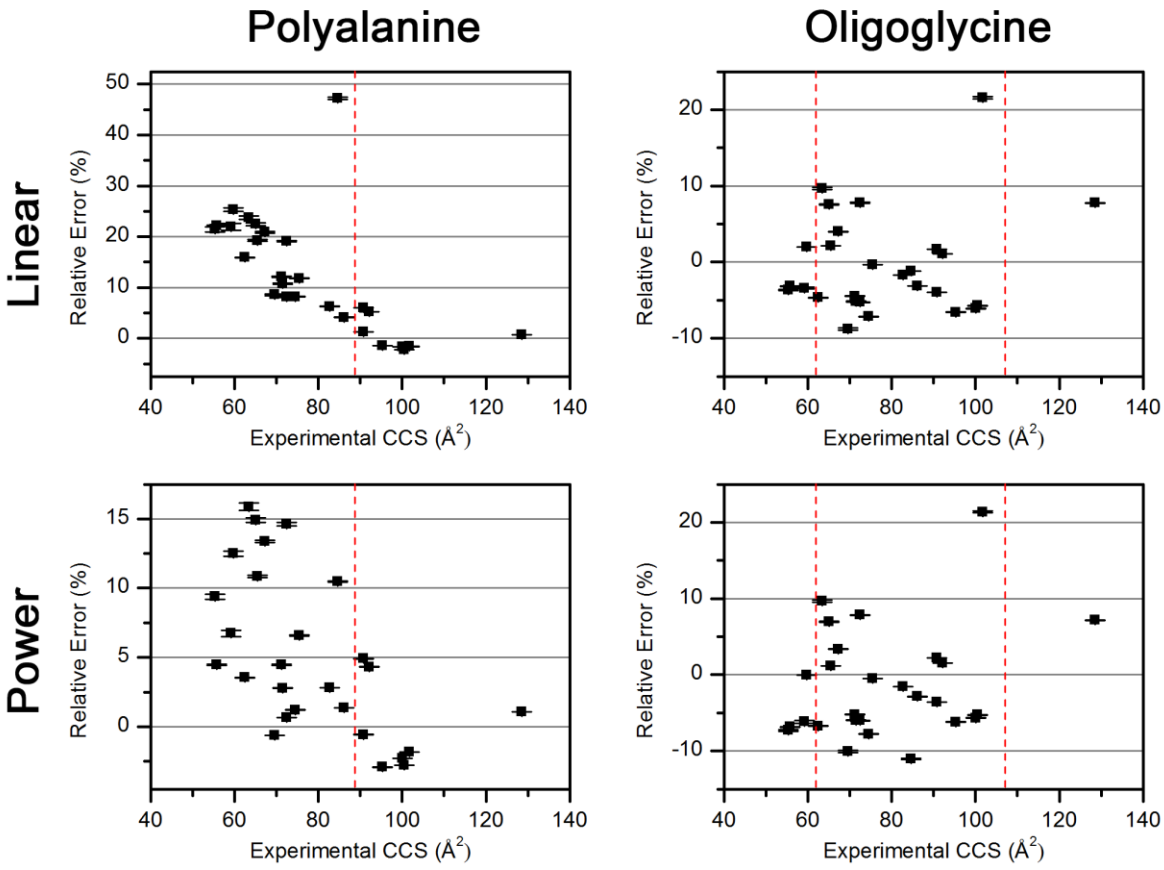

Fig. S4. Comparison of theoretical CCS values calculated using projection approximation (PA)[17] and exact hard-spheres scattering (EHSS)[18] methods implemented in MOBCAL to experimental CCS values. The inset numbers are RMSEs. The errors were calculated using propagation of error from the standard deviations. The data are summarized in Table S4.

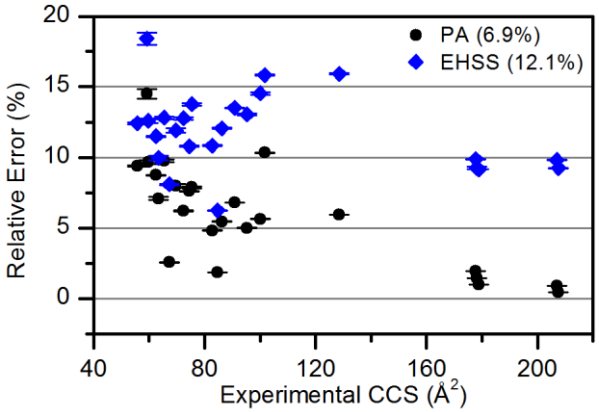

Fig. S5. a) Shapes of different LJ-type potentials (left) and Exp-6-type potentials as used in the MM3,[11] MM2,[16] and Dreiding[17] FFs (right). b) Theoretical CCS values calculated using LJ-type potentials (left) and Exp-6-type potentials (right) with scaled MMFF94 parameters. The inset numbers are RMSEs. The errors were calculated using propagation of error from the standard deviations. The data are summarized in Table S10.

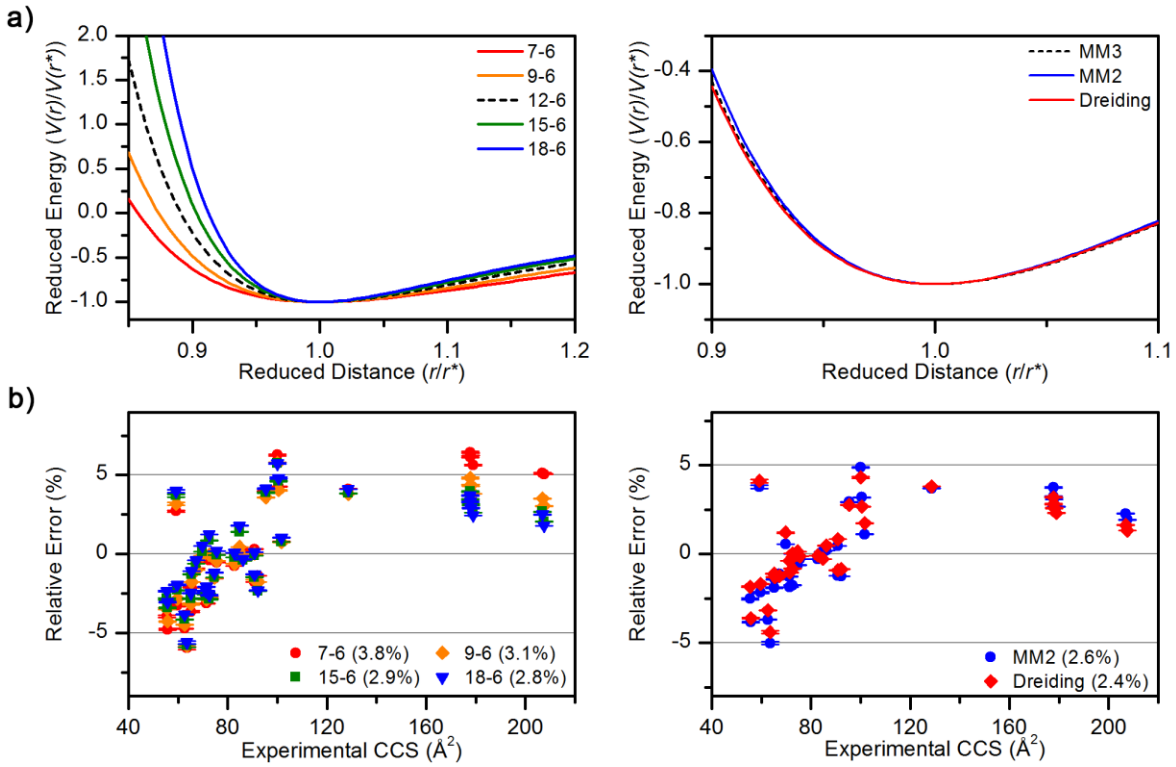

Fig. S6. Comparison between temperature-dependent experimental CCS of sodiated or potassiated 18-crown-6 (18C6) and theoretical CCS calculated using the combination of MM3 vdW potential-form and MMFF94 parameters (δ_{dist} = 0.98, δ_{ener} = 0.81). The results are presented in terms of a) absolute values and b) relative errors.

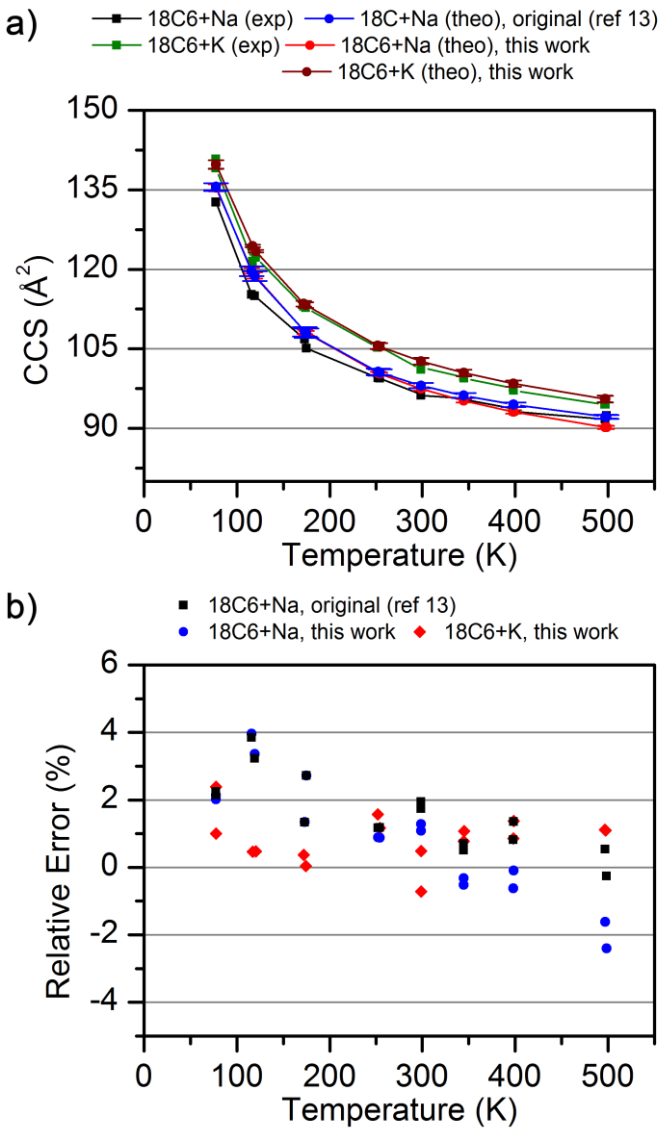

Fig. S7. Ratio of the CCS values calculated using the original TJ parameters[13] without charges or with equally-distributed partial charges to the CCS values calculated using the optimized MMFF94/Exp-6(MM3) potential without charges. The errors were calculated using propagation of error from the standard deviations. It can be seen that the deviations for larger ions are negligible.

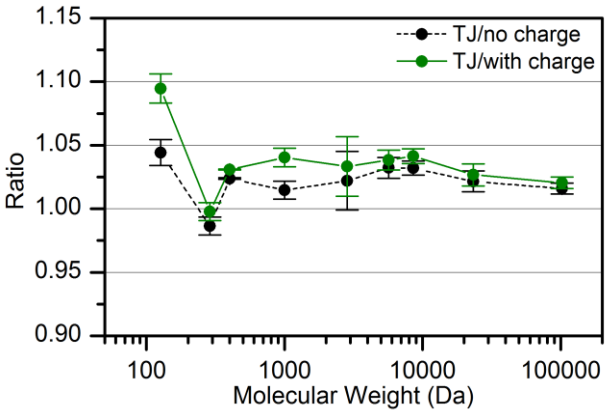

Table S1. Types of vdW potential-forms used in this study

Name of the vdW potential-form	Relevant FF	Equation
12-6 LJ	CHARMM, AMBER, CGENFF, GAFF	$V(r_i) = 4\varepsilon_i[(\frac{\sigma_i}{r_i})^{12} - (\frac{\sigma_i}{r_i})^6] = \varepsilon_i[(\frac{r_i^*}{r_i})^{12} - 2(\frac{r_i^*}{r_i})^6]$
Exp-6	MM3, MM2, Dreiding	$V(r_i) = \varepsilon_i[1.84 \times 10^5 \exp\left(-\frac{12r_i}{r_i^*}\right) - 2.25(\frac{r_i^*}{r_i})^6]$ (MM3) $V(r_i) = \varepsilon_i[2.90 \times 10^5 \exp\left(-\frac{12.5r_i}{r_i^*}\right) - 2.25(\frac{r_i^*}{r_i})^6]$ (MM2) $V(r_i) = \varepsilon_i[\exp(12.0) \exp\left(-\frac{12r_i}{r_i^*}\right) - 2(\frac{r_i^*}{r_i})^6]$ (Dreiding)
Buf-14-7	MMFF94	$V(r_i) = \varepsilon_i(\frac{1.07r_i^*}{r_i + 0.07r_i^*})^7 \left(\frac{1.12{r_i^*}^7}{{r_i}^7 + 0.12{r_i^*}^7} - 2\right)$
7-6 LJ	-	$V(r_i) = \varepsilon_i[6(\frac{r_i^*}{r_i})^7 - 7(\frac{r_i^*}{r_i})^6]$
9-6 LJ	COMPASS	$V(r_i) = \varepsilon_i[2(\frac{r_i^*}{r_i})^9 - 3(\frac{r_i^*}{r_i})^6]$
15-6 LJ	-	$V(r_i) = \varepsilon_i[\frac{2}{3}(\frac{r_i^*}{r_i})^{15} - \frac{5}{3}(\frac{r_i^*}{r_i})^6]$
18-6 LJ	-	$V(r_i) = \varepsilon_i[\frac{1}{2}(\frac{r_i^*}{r_i})^{18} - \frac{3}{2}(\frac{r_i^*}{r_i})^6]$

Table S2. Product numbers of compounds used in this study and *m/z* values for their ions. See Fig. S1 for the identity of the molecules.

No.	Supplier, product number
1	TCI, T0234
2	SA, 305065
3	SA, G11950
4	SA, A1260
5	SA, A79604
6	SA, A79809
7	SA, 36733
8	TCI, C0032
9	SA, 240931
10	SA, E4250
11	SA, 36541
12	SA, 150215
13	TCI, M2616
14	TCI, D5028
15	SA, D64600
16	SA, C4024
17	TCI, M1782
18	SA, PHR1378
19	SA, F9005
20	TCI, M0501
21	TCI, D4177
22	TCI, T3248
23	SA, C9754
24	SA, 186551
25	SA, 94544
26	SA, 545201

Table S3. Experimental ion CCS values determined from TWIM-MS experiments using either polyalanines or oligoglycines as the calibrant and a linear-fit or a power-fit calibration curve. See Fig. S1 for the identity of the molecules. The values in parentheses are percent errors with respect to CCS values measured experimentally using DTIM-MS.

No.	Form	Polyalanine, linear	Polyalanine, power	Oligoglycine, linear	Oligoglycine, power
1	H^+	68.0 (22.1)	58.2 (4.5)	54.0 (−3.1)	51.9 (−6.8)
2	H^+	72.1 (21.9)	63.1 (6.7)	57.2 (−3.4)	55.5 (−6.2)
3	H^+	74.8 (25.3)	67.1 (12.5)	60.9 (2.0)	59.6 (0.0)
4	H^+	81.3 (20.9)	76.2 (13.4)	69.9 (4.0)	69.5 (3.4)
5	H^+	72.4 (15.9)	64.7 (3.6)	59.6 (−4.7)	58.3 (−6.7)
6	H^+	78.5 (23.7)	73.2 (15.4)	69.6 (9.7)	69.6 (9.7)
7	H^+	78.3 (8.1)	72.9 (0.7)	68.6 (−5.3)	68.0 (−6.0)
8	H^+	75.6 (8.6)	69.2 (−0.6)	63.5 (−8.8)	62.6 (−10.1)
9	H^+	78.0 (19.3)	72.5 (10.8)	66.8 (2.1)	66.2 (1.1)
10	H^+	84.4 (11.8)	80.4 (6.6)	75.2 (−0.3)	75.1 (−0.5)
11	$z = 2$	124.6 (47.2)	93.6 (10.5)	83.7 (−1.2)	75.4 (−11.0)
12	H^+	80.6 (8.2)	75.4 (1.2)	69.1 (−7.1)	68.7 (−7.8)
13	H^+	79.1 (10.8)	73.4 (2.8)	67.8 (−5.2)	67.2 (−6.0)
14	H^+	88.0 (6.3)	85.1 (2.8)	81.4 (−1.7)	81.5 (−1.5)
15	H^+	79.8 (12.1)	74.4 (4.5)	68.0 (−4.5)	67.5 (−5.2)
16	H^+	89.7 (4.1)	87.3 (1.4)	83.5 (−3.1)	83.7 (−2.9)
17	H^+	92.0 (1.2)	90.3 (−0.6)	87.3 (−3.9)	87.6 (−3.6)
18	H^+	96.2 (6.0)	95.2 (4.9)	92.3 (1.7)	92.7 (2.2)
19	H^+	97.0 (5.2)	96.2 (4.3)	93.2 (1.1)	93.6 (1.5)
20	$z = 1$	100.0 (−1.6)	99.8 (−1.8)	123.6 (21.6)	123.4 (21.4)
21	H^+	86.3 (19.1)	83.1 (14.6)	78.1 (7.8)	78.2 (7.8)
22	H^+	79.7 (22.5)	74.8 (14.9)	70.0 (7.6)	69.6 (7.0)
23	H^+	129.5 (0.8)	130.0 (1.1)	138.6 (7.8)	137.8 (7.1)
24	NH_4^+ Na^+ K^+	98.3 (−1.7) 94.0 (−1.4) 98.3 (−2.2)	97.8 (−2.3) 92.6 (−2.9) 97.7 (−2.8)	94.0 (−6.1) 89.1 (−6.6) 94.8 (−5.7)	94.4 (−5.6) 89.4 (−6.2) 95.2 (−5.3)
Average percent error		12.1%	4.9%	−0.2%	−1.2%
Root-mean-square error		16.5%	7.5%	6.7%	7.2%
Percent-error range		−2.2% ~ 47.2%	−2.9% ~ 15.4%	−8.8% ~ 21.6%	−11% ~ 21.4%
Median		9.7%	4.0%	−2.4%	-3.3%

Table S4. CCS values calculated using previously reported methods.[6, 7, 13, 29, 30] See Fig. S1 for the identity of the molecules. The values in parentheses are percent errors with respect to experimental CCS values measured using DTIM-MS. N.A. = Not available because no parameters are available for one or more elements. Refs 13, 29 and 30 in the Supporting Information correspond to refs 9, 19, and 20 in the main text, respectively.

No.	Form	CCS_{PA}	CCS_{EHSS}	$CCS_{TJ,ref13}$	$CCS_{TJ,ref29}$	$CCS_{TJ,ref30}$
1	H^+	60.9 (9.4)	62.6 (12.4)	58.8 (5.6)	53.0 (−4.8)	55.8 (0.2)
2	H^+	67.7 (14.5)	70.1 (18.4)	64.7 (9.3)	58.7 (−0.7)	68.4 (15.6)
3	H^+	65.4 (9.7)	67.2 (12.6)	63.1 (5.8)	56.9 (−4.7)	65.2 (9.3)
4	H^+	69.0 (2.6)	72.7 (8.1)	66.7 (−0.8)	61.4 (−8.6)	66.0 (−1.8)
5	H^+	67.9 (8.7)	69.7 (11.5)	65.0 (4.1)	59.0 (−5.6)	62.3 (−0.3)
6	H^+	68.0 (7.1)	69.8 (10.0)	65.3 (2.8)	59.1 (−6.9)	62.7 (−1.2)
7	H^+	76.9 (6.2)	81.6 (12.8)	74.6 (3.0)	68.9 (−4.9)	73.8 (1.9)
8	H^+	75.2 (8.0)	77.9 (11.9)	71.7 (3.0)	65.5 (−5.9)	70.9 (1.8)
9	H^+	71.8 (9.8)	73.8 (12.8)	69.5 (6.3)	62.8 (−4.0)	64.2 (−1.8)
10	H^+	81.4 (7.9)	85.9 (13.8)	80.2 (6.2)	72.8 (−3.5)	74.3 (−1.5)
11	$z = 2$	86.3 (1.9)	90.0 (6.3)	88.0 (3.9)	82.1 (−3.1)	87.0 (2.7)
12	H^+	80.1 (7.6)	82.5 (10.8)	76.8 (3.1)	70.0 (−6.0)	75.5 (1.4)
13	H^+	N.A.	N.A.	N.A.	N.A.	N.A.
14	H^+	86.8 (4.8)	91.7 (10.8)	84.5 (2.1)	78.2 (−5.6)	82.9 (0.1)
15	H^+	N.A.	N.A.	N.A.	N.A.	N.A.
16	H^+	90.9 (5.5)	96.6 (12.1)	89.4 (3.7)	82.4 (−4.4)	87.7 (1.8)
17	H^+	97.0 (6.8)	103.1 (13.5)	95.4 (5.0)	87.9 (−3.3)	90.7 (−0.1)
18	H^+	N.A.	N.A.	N.A.	N.A.	92.2 (1.6)
19	H^+	N.A.	N.A.	N.A.	N.A.	91.4 (−0.9)
20	$z = 1$	112.2 (10.3)	117.8 (15.8)	105.7 (4.0)	98.6 (−3.0)	105.5 (3.8)
21	H^+	N.A.	N.A.	N.A.	N.A.	N.A.
22	H^+	N.A.	N.A.	N.A.	N.A.	N.A.
23	H^+	136.2 (5.9)	149.0 (15.9)	137.8 (7.1)	128.1 (−0.4)	132.8 (3.3)
24	NH_4^+ Na^+ K^+	105.7 (5.6) 100.1 (5.0) N.A.	114.6 (14.5) 107.8 (13.0) N.A.	104.5 (4.5) 98.1 (2.9) N.A.	98.3 (−1.7) 91.7 (−3.9) N.A.	102.3 (2.3) 96.4 (1.1) N.A.
25	$2H^+$ $Na^+ + NH_4^+$ $2Na^+$ $Na^+ + K^+$	180.7 (1.0) 181.2 (1.9) 180.7 (1.5) N.A.	195.2 (9.2) 195.3 (9.9) 194.6 (9.2) N.A.	191.0 (6.8) 189.2 (6.5) 189.3 (6.3) N.A.	179.0 (0.1) 178.1 (0.2) 177.8 (−0.2) N.A.	186.9 (4.5) 190.0 (6.9) 188.0 (5.5) N.A.
26	$2H^+$ $2Na^+$	208.9 (0.9) 208.5 (0.4)	227.3 (9.8) 226.7 (9.2)	221.2 (6.9) 218.6 (5.3)	207.3 (0.2) 205.4 (−1.0)	215.4 (4.1) 214.9 (3.6)
Average percent error		6.0%	11.8%	4.8%	−3.4%	2.5%
Root-mean-square error		6.9%	12.1%	5.2%	4.2%	4.5%
Percent-error range		0.4% ~ 14.5%	6.3% ~ 18.4%	−0.8% ~ 9.3%	−8.6% ~ 0.2%	−1.8% ~ 15.6%
Median		6.1%	12.0%	4.8%	−3.7%	1.8%

Table S5. CCS values calculated using original TJ parameters[13] and different partial charge assignment schemes. See Fig. S1 for the identity of the molecules. The values in parentheses are the ratios of the CCS values calculated using Merz-Kollman (MK), uniform, or no charges, to CCS calculated using Mulliken partial charges. N.A. = Not available because no parameters are available for one or more elements.

No.	Form	Merz-Kollman	Uniform	No charge
1	H^+	59.0 (1.004)	58.5 (0.995)	56.1 (0.954)
2	H^+	64.7 (1.000)	64.5 (0.997)	62.5 (0.966)
3	H^+	63.5 (1.005)	62.9 (0.996)	60.7 (0.961)
4	H^+	67.0 (1.005)	66.5 (0.997)	64.1 (0.961)
5	H^+	65.2 (1.002)	65.1 (1.001)	63.1 (0.970)
6	H^+	65.3 (1.001)	65.2 (1.000)	63.2 (0.969)
7	H^+	74.7 (1.002)	74.8 (1.002)	72.6 (0.974)
8	H^+	72.1 (1.005)	71.7 (1.001)	69.8 (0.973)
9	H^+	69.8 (1.004)	69.1 (0.993)	67.1 (0.964)
10	H^+	80.1 (0.999)	79.5 (0.992)	77.5 (0.967)
11	$z = 2$	88.0 (1.001)	88.3 (1.003)	80.3 (0.913)
12	H^+	77.0 (1.002)	76.8 (1.000)	75.0 (0.977)
13	H^+	N.A.	N.A.	N.A.
14	H^+	84.9 (1.005)	84.7 (1.002)	82.9 (0.981)
15	H^+	N.A.	N.A.	N.A.
16	H^+	89.6 (1.002)	89.6 (1.002)	87.9 (0.983)
17	H^+	95.7 (1.002)	95.6 (1.002)	93.9 (0.984)
18	H^+	N.A.	N.A.	N.A.
19	H^+	N.A.	N.A.	N.A.
20	$z = 1$	105.7 (1.001)	105.8 (1.001)	104.6 (0.989)
21	H^+	N.A.	N.A.	N.A.
22	H^+	N.A.	N.A.	N.A.
23	H^+	137.9 (1.001)	137.9 (1.001)	136.8 (0.993)
24	NH_4^+ Na^+ K^+	104.6 (1.001) 98.1 (0.999) N.A.	104.8 (1.003) 98.3 (1.002) N.A.	103.3 (0.989) 96.7 (0.986) N.A.
25	$2H^+$ $Na^+ + NH_4^+$ $2Na^+$ $Na^+ + K^+$	191.4 (1.002) 190.0 (1.004) 190.1 (1.004) N.A.	189.9 (0.994) 188.3 (0.995) 1883. (0.994) N.A.	186.3 (0.975) 184.6 (0.975) 184.2 (0.973) N.A.
26	$2H^+$ $2Na^+$	221.8 (1.003) 219.3 (1.002)	219.4 (0.992) 217.5 (0.995)	216.0 (0.979) 214.1 (0.976)
Average ratio		1.002	0.998	0.972
Root-mean-square ratio		1.002	0.998	0.972
Ratio range		0.999 ~ 1.005	0.992 ~ 1.003	0.913 ~ 0.993
Median		1.002	1.000	0.974

Table S6. CCS values calculated using unmodified FF vdW potentials. See Fig. S1 for the identity of the molecules. The values in parentheses are percent errors with respect to experimental CCS values measured using DTIM-MS. N.A. = Not available because no parameters are available for one or more elements.

No.	Form	CCS_{CGENFF}	CCS_{GAFF}	CCS_{MM3}	CCS_{MMFF94}
1	H^+	62.6 (12.4)	62.3 (11.8)	62.1 (11.4)	59.8 (7.3)
2	H^+	66.8 (12.9)	65.4 (10.5)	71.6 (21.1)	68.2 (15.3)
3	H^+	64.9 (8.8)	65.1 (9.2)	66.6 (11.7)	65.3 (9.4)
4	H^+	73.0 (8.6)	72.9 (8.4)	74.3 (10.5)	73.4 (9.2)
5	H^+	68.3 (9.3)	67.2 (7.6)	69.6 (11.4)	67.2 (7.5)
6	H^+	68.4 (7.9)	67.5 (6.3)	69.7 (9.9)	67.3 (6.1)
7	H^+	82.1 (13.4)	81.0 (11.9)	82.8 (14.4)	79.7 (10.1)
8	H^+	78.6 (12.9)	77.1 (10.7)	80.0 (14.9)	77.8 (11.7)
9	H^+	73.8 (12.8)	73.5 (12.3)	72.8 (11.3)	71.4 (9.1)
10	H^+	86.3 (14.3)	82.3 (9.0)	85.8 (13.7)	82.8 (9.7)
11	$z = 2$	97.0 (14.5)	94.1 (11.1)	95.3 (12.6)	92.6 (9.3)
12	H^+	83.6 (12.3)	82.9 (11.3)	84.2 (13.1)	82.3 (10.5)
13	H^+	79.6 (11.4)	78.4 (9.8)	79.9 (11.9)	78.5 (9.8)
14	H^+	92.7 (11.9)	91.5 (10.5)	94.3 (13.9)	90.7 (9.6)
15	H^+	79.6 (11.9)	77.6 (9.0)	80.0 (12.4)	78.5 (10.3)
16	H^+	97.1 (12.7)	96.6 (12.2)	98.4 (14.2)	94.5 (9.7)
17	H^+	103.3 (13.7)	102.3 (12.6)	103.7 (14.1)	100.3 (10.4)
18	H^+	102.8 (13.2)	103.1 (13.6)	102.3 (12.8)	98.6 (8.6)
19	H^+	104.0 (12.9)	102.9 (11.6)	103.9 (12.8)	99.9 (8.4)
20	$z = 1$	116.6 (14.7)	112.8 (10.9)	115.8 (13.9)	112.8 (10.9)
21	H^+	79.7 (10.0)	77.8 (7.3)	81.0 (11.8)	79.6 (9.7)
22	H^+	72.4 (11.3)	70.2 (7.9)	74.2 (14.1)	71.9 (10.5)
23	H^+	149.4 (16.2)	148.4 (15.5)	151.0 (17.4)	144.2 (12.2)
24	NH_4^+ Na^+ K^+	116.0 (16.0) 109.4 (14.8) 115.9 (15.3)	113.9 (13.9) 107.2 (12.4) 113.0 (12.4)	116.8 (16.7) N.A. N.A.	112.7 (12.6) 106.1 (11.2) 111.6 (11.0)
25	$2H^+$ $Na^+ + NH_4^+$ $2Na^+$ $Na^+ + K^+$	205.0 (14.6) 204.4 (15.0) 204.1 (14.6) 204.4 (15.0)	203.1 (13.5) 201.7 (13.5) 201.5 (13.1) 201.3 (13.2)	200.5 (12.1) N.A. N.A. N.A.	194.2 (8.6) 194.5 (9.4) 193.8 (8.8) 193.4 (8.8)
26	$2H^+$ $2Na^+$	235.7 (13.9) 234.3 (12.9)	234.1 (13.7) 231.8 (11.7)	231.2 (11.7) N.A.	223.6 (8.0) 222.5 (7.2)
Average percent error		12.9%	11.2%	13.3%	9.7%
Root-mean-square error		13.2%	11.6%	13.5%	9.9%
Percent-error range		7.9% ~ 16.2%	6.3% ~ 15.5%	9.9 ~ 21.1%	6.1% ~ 15.3%
Median		12.9%	11.7%	12.8%	9.7%

Table S7. CCS values calculated using uniformly-scaled FF vdW parameters. See Fig. S1 for the identity of the molecules. The values in parentheses are percent errors with respect to experimental CCS values measured using DTIM-MS. N.A. = Not available because no parameters are available for one or more elements.

No.	Form	CCS_{CGENFF} $\delta_{dist} = 0.91$ $\delta_{ener} = 0.80$	CCS_{GAFF} $\delta_{dist} = 0.91$ $\delta_{ener} = 0.85$	CCS_{MM3} $\delta_{dist} = 0.90$ $\delta_{ener} = 0.85$	CCS_{MMFF94} $\delta_{dist} = 0.93$ $\delta_{ener} = 0.91$
1	H^+	54.6 (−2.0)	56.1 (0.7)	53.6 (−3.7)	54.1 (−2.9)
2	H^+	58.2 (−1.7)	58.6 (−0.9)	62.3 (5.3)	61.5 (4.0)
3	H^+	56.3 (−5.7)	58.1 (−2.7)	57.6 (−3.5)	58.5 (−2.0)
4	H^+	65.2 (−3.0)	65.8 (−2.2)	65.4 (−2.8)	66.5 (−1.1)
5	H^+	59.6 (−4.6)	60.3 (−3.4)	60.1 (−3.8)	60.4 (−3.3)
6	H^+	59.7 (−6.0)	60.8 (−4.2)	60.1 (−5.3)	60.5 (−4.7)
7	H^+	73.0 (0.9)	73.0 (0.9)	72.9 (0.7)	73.4 (1.3)
8	H^+	68.9 (−1.0)	69.1 (−0.7)	69.6 (−0.1)	70.4 (1.1)
9	H^+	64.9 (−0.8)	66.3 (1.4)	63.7 (−2.7)	64.5 (−1.4)
10	H^+	76.3 (1.1)	74.2 (−1.7)	75.3 (−0.3)	75.8 (0.4)
11	$z = 2$	86.7 (2.4)	85.5 (1.0)	84.5 (−0.2)	85.6 (1.0)
12	H^+	73.7 (−1.0)	74.3 (−0.2)	73.1 (−1.8)	74.4 (−0.1)
13	H^+	69.8 (−2.3)	69.9 (−2.2)	69.1 (−3.4)	70.8 (−0.9)
14	H^+	82.3 (−0.6)	82.3 (−0.5)	83.0 (0.3)	83.1 (0.3)
15	H^+	69.6 (−2.2)	68.7 (−3.4)	69.1 (−3.0)	70.7 (−0.7)
16	H^+	86.5 (0.4)	87.3 (1.3)	86.6 (0.6)	86.4 (0.3)
17	H^+	91.8 (1.0)	92.4 (1.7)	91.1 (0.3)	92.0 (1.3)
18	H^+	91.4 (0.7)	93.1 (2.6)	90.0 (−0.9)	90.1 (−0.7)
19	H^+	92.1 (0.0)	92.4 (0.2)	90.9 (−1.3)	91.5 (−0.7)
20	$z = 1$	103.7 (2.0)	101.8 (0.1)	102.2 (0.6)	103.7 (2.0)
21	H^+	69.7 (−3.8)	68.9 (−4.9)	69.8 (−3.7)	71.4 (−1.5)
22	H^+	62.8 (−3.5)	61.8 (−5.1)	63.4 (−2.5)	64.3 (−1.2)
23	H^+	134.6 (4.7)	135.1 (5.1)	134.9 (4.9)	133.6 (3.9)
24	NH_4^+ Na^+ K^+	105.6 (5.5) 98.9 (3.7) 105.5 (5.0)	104.7 (4.7) 97.6 (2.4) 104.4 (3.9)	104.9 (4.9) N.A. N.A.	104.6 (4.6) 97.8 (2.6) 103.6 (3.0)
25	$2H^+$ $Na^+ + NH_4^+$ $2Na^+$ $Na^+ + K^+$	187.2 (4.7) 187.4 (5.4) 186.9 (4.9) 187.3 (5.3)	187.7 (5.0) 186.9 (5.1) 187.0 (5.0) 186.5 (4.9)	181.9 (1.7) N.A. N.A. N.A.	181.9 (1.7) 182.8 (2.8) 181.6 (1.9) 181.9 (2.3)
26	$2H^+$ $2Na^+$	216.2 (4.4) 215.2 (3.7)	217.7 (5.2) 216.0 (4.1)	211.1 (2.0) N.A.	210.1 (1.5) 209.4 (0.9)
Average percent error		0.6%	0.7%	−0.7%	0.5%
Root-mean-square error		3.5%	3.1%	2.9%	2.4%
Percent-error range		−6.0% ~ 5.5%	−5.1% ~ 5.2%	−5.3% ~ 5.3%	−4.7% ~ 4.6%
Median		0.6%	0.8%	−0.6%	0.7%

Table S8. Summary of vdW parameters and potential-form combinations used in this study. Original usage in FFs are noted.

VdW potential form	Tested FF parameters	Relevant figures/tables
12-6 LJ	CGENFF (original)	Fig. 3, Table S6, S7
	GAFF (original)	Fig. 3, Table S6, S7
	MM3	Fig. 4, Table S9
	MMFF94	Fig. 4, Table S9
Exp-6(MM3)	CGENFF	Fig. 4, Table S9
	MM3 (original)	Fig. 3, Table S6, S7
	MMFF94	Figs. 4, 5, S6, S7 Table S9
Buf-14-7	CGENFF	Fig. 4, Table S9
	GAFF	Fig. 4, Table S9
	MM3	Fig. 4, Table S9
	MMFF94 (original)	Fig. 3, Table S6, S7
7-6 LJ	MMFF94	Fig. S5, Table S10
9-6 LJ	MMFF94	Fig. S5, Table S10
15-6 LJ	MMFF94	Fig. S5, Table S10
18-6 LJ	MMFF94	Fig. S5, Table S10
Exp-6(MM2)	MMFF94	Fig. S5, Table S10
Exp-6(Dreiding)	MMFF94	Fig. S5, Table S10

Table S9. CCS values calculated using different combinations of vdW potential and FF parameters. See Fig. S1 for the identity of the molecules. The values in parentheses are percent errors with respect to experimental CCS values measured using DTIM-MS. N.A. = Not available because no parameters are available for one or more elements.

No.	Form	12-6 LJ		Buf-14-7			Exp-6(MM3)	
		CCS_{MM3}	CCS_{MMFF94}	CCS_{CGENFF}	CCS_{GAFF}	CCS_{MM3}	CCS_{CGENFF}	CCS_{MMFF94}
		δ_{dist} = 0.82 δ_{ener} = 0.82	δ_{dist} = 0.88 δ_{ener} = 0.86	δ_{dist} = 0.91 δ_{ener} = 1.09	δ_{dist} = 0.93 δ_{ener} = 0.97	δ_{dist} = 0.82 δ_{ener} = 1.15	δ_{dist} = 0.99 δ_{ener} = 0.81	δ_{dist} = 0.98 δ_{ener} = 0.81
1	H^+	53.7 (−3.7)	53.8 (−3.5)	55.2 (−0.9)	55.2 (−0.9)	53.7 (−3.6)	55.0 (−1.4)	53.7 (−3.6)
2	H^+	62.3 (5.2)	61.4 (3.8)	58.9 (−0.5)	58.4 (−1.2)	62.3 (5.2)	58.7 (−0.8)	61.6 (4.2)
3	H^+	57.6 (−3.5)	58.4 (−2.2)	56.9 (−4.6)	58.3 (−2.3)	57.6 (−3.5)	56.9 (−4.7)	58.7 (−1.7)
4	H^+	66.1 (−1.8)	66.8 (−0.7)	65.2 (−3.0)	64.7 (−3.8)	65.9 (−2.0)	64.6 (−4.0)	66.6 (−1.0)
5	H^+	59.7 (−4.5)	60.0 (−4.0)	60.2 (−3.6)	60.4 (−3.3)	59.9 (−4.2)	60.0 (−3.9)	60.5 (−3.2)
6	H^+	59.6 (−6.1)	60.0 (−5.5)	60.3 (−4.9)	60.5 (−4.7)	59.8 (−5.8)	60.2 (−5.1)	60.6 (−4.4)
7	H^+	73.4 (1.5)	72.9 (0.6)	73.2 (1.1)	71.8 (−0.9)	73.4 (1.4)	72.6 (0.3)	72.5 (0.2)
8	H^+	69.3 (−0.5)	69.9 (0.4)	69.4 (−0.3)	68.4 (−1.7)	69.3 (−0.4)	69.5 (−0.2)	70.4 (1.1)
9	H^+	63.8 (−2.5)	64.6 (−1.3)	65.4 (−0.1)	66.7 (1.9)	63.9 (−2.3)	65.1 (−0.4)	64.7 (−1.2)
10	H^+	75.5 (0.0)	75.4 (0.0)	76.9 (1.9)	73.2 (−3.0)	75.4 (−0.1)	76.6 (1.5)	75.5 (0.0)
11	$z = 2$	85.6 (1.1)	85.6 (1.1)	86.7 (2.4)	83.5 (−1.4)	85.2 (0.6)	86.2 (1.8)	84.7 (0.0)
12	H^+	72.5 (−2.6)	73.6 (−1.1)	74.0 (−0.6)	73.5 (−1.3)	72.7 (−2.4)	74.0 (−0.6)	74.5 (0.0)
13	H^+	68.1 (−4.7)	69.9 (−2.2)	70.5 (−1.4)	69.9 (−2.1)	68.7 (−3.8)	70.6 (−1.3)	70.6 (−1.2)
14	H^+	82.8 (0.1)	82.6 (−0.1)	82.6 (−0.2)	81.3 (−1.8)	82.9 (0.1)	82.5 (−0.3)	82.8 (0.0)
15	H^+	67.7 (−4.8)	69.7 (−2.0)	70.5 (−1.0)	68.7 (−3.4)	68.4 (−3.9)	70.8 (−0.5)	70.8 (−0.5)
16	H^+	86.3 (0.2)	86.1 (−0.1)	86.9 (0.8)	87.1 (1.0)	86.6 (0.5)	86.6 (0.5)	86.7 (0.6)
17	H^+	90.7 (−0.2)	91.0 (0.2)	92.3 (1.6)	90.7 (−0.2)	90.9 (0.1)	92.3 (1.6)	91.7 (0.9)
18	H^+	89.7 (−1.2)	89.6 (−1.3)	91.9 (1.2)	91.9 (1.2)	90.0 (−0.8)	91.6 (0.9)	90.0 (−0.8)
19	H^+	89.9 (−2.5)	90.4 (−1.9)	92.8 (0.7)	91.0 (−1.2)	90.3 (−2.1)	92.9 (0.8)	91.5 (−0.8)
20	$z = 1$	102.2 (0.5)	102.7 (1.0)	104.0 (2.3)	100.0 (−1.6)	102.0 (0.3)	104.4 (2.7)	103.4 (1.7)
21	H^+	68.3 (−5.8)	70.8 (−2.4)	70.7 (−2.5)	69.6 (−4.0)	69.2 (−4.6)	70.9 (−2.2)	71.8 (−1.0)
22	H^+	61.7 (−5.2)	63.5 (−2.5)	64.1 (−1.6)	62.5 (−3.9)	62.9 (−3.4)	64.1 (−1.5)	64.3 (−1.2)
23	H^+	134.8 (4.9)	133.5 (3.9)	134.8 (4.8)	133.8 (4.1)	134.6 (4.7)	134.7 (4.8)	133.6 (3.9)
24	NH_4^+ Na^+ K^+	105.7 (5.6) N.A. N.A.	105.7 (5.7) 98.9 (3.7) 104.8 (4.3)	105.4 (5.4) 98.7 (3.6) 105.4 (4.8)	103.3 (3.3) 96.1 (0.8) 105.4 (4.9)	105.3 (5.2) N.A. N.A.	104.8 (4.8) 98.5 (3.3) 104.6 (4.1)	104.7 (4.7) 98.2 (3.0) 103.5 (3.0)
25	$2H^+$ $Na^+ + NH_4^+$ $2Na^+$ $Na^+ + K^+$	182.7 (2.1) N.A. N.A. N.A.	183.7 (2.7) 184.9 (4.0) 184.1 (3.3) 184.0 (3.5)	187.1 (4.6) 186.7 (5.1) 186.5 (4.7) 186.7 (5.0)	185.4 (3.6) 184.3 (3.7) 184.9 (3.8) 184.1 (3.5)	181.9 (1.7) N.A. N.A. N.A.	188.2 (5.2) 188.3 (5.9) 187.9 (5.5) 187.8 (5.6)	183.6 (2.7) 184.2 (3.7) 183.5 (3.0) 183.6 (3.2)
26	$2H^+$ $2Na^+$	212.5 (2.7) N.A.	212.6 (2.7) 212.1 (2.2)	216.0 (4.7) 214.9 (3.5)	213.6 (3.2) 213.2 (2.7)	211.3 (2.1) N.A.	216.8 (4.7) 215.7 (3.9)	211.7 (2.3) 211.2 (1.8)
Average percent error		−1.0%	0.4%	1.0%	−0.2%	−0.8%	1.0%	0.6%
Root-mean-square error		3.5%	2.8%	3.3%	2.7%	3.1%	3.4%	2.5%
Percent error range		−6.1% ~ 5.6%	−5.5% ~ 5.7%	−4.9% ~ 5.4%	−4.7% ~ 4.9%	−5.8% ~ 5.2%	−5.1% ~ 5.9%	−4.4% ~ 4.7%
Median		−0.9%	0.1%	1.0%	−1.1%	−0.6%	0.7%	0.1%

Table S10. CCS values calculated using combinations of the MMFF94 parameters with different vdW potential-forms. See Fig. S1 for the identity of the molecules. The values in parentheses are percent errors with respect to experimental CCS values measured using DTIM-MS.

No.	Form	MMFF94					
		7-6 LJ	9-6 LJ	15-6 LJ	18-6 LJ	Exp-6 (MM2)	Exp-6 (Dreiding)
		δ_{dist} = 0.97 δ_{ener} = 0.82	δ_{dist} = 0.92 δ_{ener} = 0.88	δ_{dist} = 0.83 δ_{ener} = 0.97	δ_{dist} = 0.82 δ_{ener} = 0.82	δ_{dist} = 0.94 δ_{ener} = 0.89	δ_{dist} = 1.00 δ_{ener} = 0.81
1	H^+	53.1 (−4.8)	53.3 (−4.3)	53.8 (−3.4)	54.0 (−3.0)	53.6 (−3.8)	53.7 (−3.6)
2	H^+	60.8 (2.7)	61.0 (3.2)	61.4 (3.7)	61.5 (4.0)	61.4 (3.8)	61.6 (4.1)
3	H^+	57.7 (−3.3)	58.0 (−2.9)	58.3 (−2.3)	58.5 (−1.9)	58.4 (−2.2)	58.7 (−1.7)
4	H^+	66.6 (−0.9)	66.6 (−1.0)	66.8 (−0.6)	67.0 (−0.4)	66.5 (−1.1)	66.4 (−1.2)
5	H^+	59.5 (−4.7)	59.7 (−4.5)	59.9 (−4.1)	60.1 (−3.8)	60.2 (−3.7)	60.5 (−3.2)
6	H^+	59.7 (−6.0)	59.8 (−5.8)	59.8 (−5.8)	59.9 (−5.6)	60.3 (−5.0)	60.7 (−4.4)
7	H^+	72.1 (−0.4)	72.4 (−0.1)	73.0 (0.9)	73.3 (1.2)	72.4 (0.0)	72.4 (0.0)
8	H^+	69.4 (−0.3)	69.5 (−0.1)	69.7 (0.1)	70.0 (0.5)	70.0 (0.6)	70.5 (1.2)
9	H^+	64.0 (−2.1)	64.3 (−1.8)	64.6 (−1.3)	64.7 (−1.1)	64.5 (−1.4)	64.6 (−1.3)
10	H^+	75.1 (−0.5)	75.1 (−0.4)	75.4 (−0.1)	75.6 (0.2)	75.3 (−0.3)	75.4 (−0.1)
11	$z = 2$	84.7 (0.0)	85.1 (0.5)	85.9 (1.4)	86.2 (1.8)	84.8 (0.1)	84.5 (−0.3)
12	H^+	73.3 (−1.5)	73.3 (−1.5)	73.4 (−1.5)	73.6 (−1.2)	74.0 (−0.6)	74.6 (0.1)
13	H^+	69.2 (−3.1)	69.4 (−2.9)	69.7 (−2.5)	70.0 (−2.1)	70.1 (−1.9)	70.7 (−1.0)
14	H^+	82.1 (−0.7)	82.3 (−0.6)	82.6 (−0.2)	82.8 (0.1)	82.5 (−0.3)	82.7 (−0.1)
15	H^+	69.5 (−2.4)	69.5 (−2.4)	69.4 (−2.5)	69.5 (−2.3)	70.3 (−1.3)	70.9 (−0.4)
16	H^+	86.4 (0.2)	86.1 (−0.1)	85.8 (−0.4)	85.9 (−0.3)	86.3 (0.2)	86.6 (0.5)
17	H^+	91.1 (0.3)	90.9 (0.0)	90.8 (−0.1)	91.0 (0.1)	91.3 (0.5)	91.6 (0.8)
18	H^+	89.2 (−1.8)	89.3 (−1.6)	89.4 (−1.5)	89.6 (−1.3)	89.7 (−1.2)	89.9 (−0.9)
19	H^+	90.9 (−1.4)	90.5 (−1.8)	90.0 (−2.3)	90.1 (−2.3)	91.0 (−1.2)	91.4 (−0.8)
20	$z = 1$	102.5 (0.8)	102.4 (0.7)	102.5 (0.8)	102.7 (1.0)	102.8 (1.1)	103.4 (1.7)
21	H^+	70.5 (−2.8)	70.5 (−2.7)	70.4 (−2.9)	70.6 (−2.6)	71.2 (−1.8)	71.9 (−0.8)
22	H^+	62.7 (−3.6)	63.0 (−3.2)	63.2 (−2.8)	63.5 (−2.5)	63.8 (−1.9)	64.4 (−1.1)
23	H^+	133.9 (4.1)	133.5 (3.8)	133.5 (3.8)	133.9 (4.1)	133.3 (3.7)	133.5 (3.8)
24	NH_4^+ Na^+ K^+	106.3 (6.3) 99.1 (4.0) 104.8 (4.3)	105.8 (5.8) 98.8 (3.6) 104.6 (4.0)	105.8 (5.7) 99.1 (3.9) 105.2 (4.6)	105.8 (5.7) 99.3 (4.1) 105.4 (4.8)	104.9 (4.9) 98.1 (2.9) 103.7 (3.2)	104.4 (4.3) 98.0 (2.8) 103.2 (2.7)
25	$2H^+$ $Na^+ + NH_4^+$ $2Na^+$ $Na^+ + K^+$	188.9 (5.6) 189.2 (6.4) 189.4 (6.3) 188.8 (6.1)	185.7 (3.8) 186.3 (4.8) 185.9 (4.4) 185.6 (4.4)	183.5 (2.6) 184.8 (4.0) 183.7 (3.1) 184.0 (3.5)	183.2 (2.4) 184.4 (3.7) 183.3 (2.9) 183.7 (3.3)	183.6 (2.7) 184.4 (3.7) 183.7 (3.1) 183.6 (3.2)	183.0 (2.3) 183.4 (3.2) 182.8 (2.6) 182.8 (2.8)
26	$2H^+$ $2Na^+$	217.6 (5.1) 218.1 (5.1)	214.3 (3.5) 213.9 (3.0)	212.6 (2.7) 211.8 (2.1)	212.2 (2.5) 211.3 (1.8)	211.7 (2.3) 211.6 (1.9)	210.4 (1.6) 210.3 (1.3)
Average percent error		0.5%	0.2%	0.3%	0.4%	0.3%	0.5%
Root-mean-square error		3.8%	3.1%	2.9%	2.8%	2.6%	2.4%
Percent-error range		−6.0% ~ 6.4%	−5.8% ~ 5.8%	−5.8% ~ 5.7%	−5.6 ~ 5.7%	−5.0% ~ 4.9%	−4.4% ~ 4.3%
Median		−0.4%	−0.1%	−0.1%	0.2%	0.1%	0.1%

REFERENCES

1. M. F. Bush, I. D. G. Campuzano and C. V. Robinson, *Anal. Chem.*, 2012, **84**, 7124-7130.
2. T. Wyttenbach, J. E. Bushnell and M. T. Bowers, *J. Am. Chem. Soc.*, 1998, **120**, 5098-5103.
3. M. D. Hanwell, D. E. Curtis, D. C. Lonie, T. Vandermeersch, E. Zurek and G. R. Hutchison, *J. Cheminform.*, 2012, **4**, 1-17.
4. Y. Shao, Z. Gan, E. Epifanovsky, A. T. B. Gilbert, M. Wormit, J. Kussmann, A. W. Lange, A. Behn, J. Deng, X. Feng, D. Ghosh, M. Goldey, P. R. Horn, L. D. Jacobson, I. Kaliman, R. Z. Khaliullin, T. Kuś, A. Landau, J. Liu, E. I. Proynov, Y. M. Rhee, R. M. Richard, M. A. Rohrdanz, R. P. Steele, E. J. Sundstrom, H. L. Woodcock, P. M. Zimmerman, D. Zuev, B. Albrecht, E. Alguire, B. Austin, G. J. O. Beran, Y. A. Bernard, E. Berquist, K. Brandhorst, K. B. Bravaya, S. T. Brown, D. Casanova, C.-M. Chang, Y. Chen, S. H. Chien, K. D. Closser, D. L. Crittenden, M. Diedenhofen, R. A. DiStasio, H. Do, A. D. Dutoi, R. G. Edgar, S. Fatehi, L. Fusti-Molnar, A. Ghysels, A. Golubeva-Zadorozhnaya, J. Gomes, M. W. D. Hanson-Heine, P. H. P. Harbach, A. W. Hauser, E. G. Hohenstein, Z. C. Holden, T.-C. Jagau, H. Ji, B. Kaduk, K. Khistyaev, J. Kim, J. Kim, R. A. King, P. Klunzinger, D. Kosenkov, T. Kowalczyk, C. M. Krauter, K. U. Lao, A. D. Laurent, K. V. Lawler, S. V. Levchenko, C. Y. Lin, F. Liu, E. Livshits, R. C. Lochan, A. Luenser, P. Manohar, S. F. Manzer, S.-P. Mao, N. Mardirossian, A. V. Marenich, S. A. Maurer, N. J. Mayhall, E. Neuscamman, C. M. Oana, R. Olivares-Amaya, D. P. O'Neill, J. A. Parkhill, T. M. Perrine, R. Peverati, A. Prociuk, D. R. Rehn, E. Rosta, N. J. Russ, S. M. Sharada, S. Sharma, D. W. Small, A. Sodt, T. Stein, D. Stück, Y.-C. Su, A. J. W. Thom, T. Tsuchimochi, V. Vanovschi, L. Vogt, O. Vydrov, T. Wang, M. A. Watson, J. Wenzel, A. White, C. F. Williams, J. Yang, S. Yeganeh, S. R. Yost, Z.-Q. You, I. Y. Zhang, X. Zhang, Y. Zhao, B. R. Brooks, G. K. L. Chan, D. M. Chipman, C. J. Cramer, W. A. Goddard, M. S. Gordon, W. J. Hehre, A. Klamt, H. F. Schaefer, M. W. Schmidt, C. D. Sherrill, D. G. Truhlar, A. Warshel, X. Xu, A. Aspuru-Guzik, R. Baer, A. T. Bell, N. A. Besley, J.-D. Chai, A. Dreuw, B. D. Dunietz, T. R. Furlani, S. R. Gwaltney, C.-P. Hsu, Y. Jung, J. Kong, D. S. Lambrecht, W. Liang, C. Ochsenfeld, V. A. Rassolov, L. V. Slipchenko, J. E. Subotnik, T. Van Voorhis, J. M. Herbert, A. I. Krylov, P. M. W. Gill and M. Head-Gordon, *Mol. Phys.*, 2015, **113**, 184-215.
5. B. Hess, C. Kutzner, D. van der Spoel and E. Lindahl, *J. Chem. Theory Comput.*, 2008, **4**, 435-447.
6. G. von Helden, T. Wyttenbach and M. T. Bowers, *Int. J. Mass Spectrom. Ion Processes*, 1995, **146**, 349-364.
7. A. A. Shvartsburg and M. F. Jarrold, *Chem. Phys. Lett.*, 1996, **261**, 86-91.
8. J. Wang, W. Wang, P. A. Kollman and D. A. Case, *J. Mol. Graph. Model.*, 2006, **25**, 247-260.
9. F.-Y. Dupradeau, A. Pigache, T. Zaffran, C. Savineau, R. Lelong, N. Grivel, D. Lelong, W. Rosanski and P. Cieplak, *Phys. Chem. Chem. Phys.*, 2010, **12**, 7821-7839.
10. E. Vanquelef, S. Simon, G. Marquant, E. Garcia, G. Klimerak, J. C. Delepine, P. Cieplak and F.-Y. Dupradeau, *Nucleic Acids Res.*, 2011, **39**, W511-W517.
11. N. L. Allinger, Y. H. Yuh and J. H. Lii, *J. Am. Chem. Soc.*, 1989, **111**, 8551-8566.
12. T. A. Halgren, *J. Comput. Chem.*, 1996, **17**, 490-519.
13. M. F. Mesleh, J. M. Hunter, A. A. Shvartsburg, G. C. Schatz and M. F. Jarrold, *J. Phys. Chem.*, 1996, **100**, 16082-16086.

14. T. A. Halgren, *J. Am. Chem. Soc.*, 1992, **114**, 7827-7843.
15. H. Sun, *J. Phys. Chem. B*, 1998, **102**, 7338-7364.
16. N. L. Allinger, *J. Am. Chem. Soc.*, 1977, **99**, 8127-8134.
17. S. L. Mayo, B. D. Olafson and W. A. Goddard, *J. Phys. Chem.*, 1990, **94**, 8897-8909.
18. W. Humphrey, A. Dalke and K. Schulten, *J. Mol. Graphics*, 1996, **14**, 33-38.
19. N. M. O'Boyle, M. Banck, C. A. James, C. Morley, T. Vandermeersch and G. R. Hutchison, *J. Cheminform.*, 2011, **3**, 1-14.
20. P. Tosco, T. Balle and F. Shiri, *J. Mol. Modeling*, 2011, **17**, 3021-3023.
21. M. F. Bush, Z. Hall, K. Giles, J. Hoyes, C. V. Robinson and B. T. Ruotolo, *Anal. Chem.*, 2010, **82**, 9557-9565.
22. K. Thalassinos, M. Grabenauer, S. E. Slade, G. R. Hilton, M. T. Bowers and J. H. Scrivens, *Anal. Chem.*, 2009, **81**, 248-254.
23. H. I. Kim, H. Kim, E. S. Pang, E. K. Ryu, L. W. Beegle, J. A. Loo, W. A. Goddard and I. Kanik, *Anal. Chem.*, 2009, **81**, 8289-8297.
24. C. Bleiholder, N. R. Johnson, S. Contreras, T. Wyttenbach and M. T. Bowers, *Anal. Chem.*, 2015, **87**, 7196-7203.
25. T. W. Knapman, J. T. Berryman, I. Campuzano, S. A. Harris and A. E. Ashcroft, *Int. J. Mass Spectrom.*, 2010, **298**, 17-23.
26. J. C. May, C. R. Goodwin, N. M. Lareau, K. L. Leaptrot, C. B. Morris, R. T. Kurulugama, A. Mordehai, C. Klein, W. Barry, E. Darland, G. Overney, K. Imatani, G. C. Stafford, J. C. Fjeldsted and J. A. McLean, *Anal. Chem.*, 2014, **86**, 2107-2116.
27. R. T. Kurulugama, E. Darland, F. Kuhlmann, G. Stafford and J. Fjeldsted, *Analyst*, 2015, **140**, 6834-6844.
28. S. J. Allen, K. Giles, T. Gilbert and M. F. Bush, *Analyst*, 2016, **141**, 884-891.
29. C.-K. Siu, Y. Guo, I. S. Saminathan, A. C. Hopkinson and K. W. M. Siu, *J. Phys. Chem. B*, 2010, **114**, 1204-1212.
30. I. Campuzano, M. F. Bush, C. V. Robinson, C. Beaumont, K. Richardson, H. Kim and H. I. Kim, *Anal. Chem.*, 2012, **84**, 1026-1033.